

INTEGRATIVE ANALYSIS OF LOW-CYCLE FATIGUE AND CRACK PROPAGATION IN TURBINE BLADES

Nhat Minh HOANG¹, Minh Duc HA¹, Tien Quyet NGUYEN¹, Phi Minh NGUYEN¹

¹Viettel Aerospace Institute, Hoa Lac Hi-Tech Park, Hanoi 100000, Vietnam

Abstract

This paper presents a comprehensive analysis of low cycle fatigue in turbine blades within a small turbojet engine using the finite element method. The study combines numerical simulations with experimental validation, providing a holistic understanding of crack initiation, propagation, and subsequent damage. Employing an innovative multi-model strategy with dynamic inputs from the combustor exit, the study investigates transient stress variations throughout the engine test cycle. Observations reveal heightened stress concentrations at the leading edge and localized plastic strain during ignition. The occurrence of localized plastic deformation is identified as a potential precursor to initial crack initiation, contributing to turbine blade fatigue failure. Utilizing the Manson-Coffin equation, the study successfully estimates cycles to failure based on observed local plastic strain levels. Numerical simulations, employing the Extended Finite Element Method (XFEM), accurately replicate initial crack propagation, aligning with experimental observations. Scanning microscopy analyzes the fracture surface, visually validating fatigue-related damage.

This integrated approach, harmonizing numerical predictions with experimental validation, advances understanding in turbine blade durability. Insights from this study inform design optimization and maintenance strategies for turbine blades exposed to cyclic loading during engine start-up conditions.

Keywords: Low cycle fatigue, gas turbine engine, turbine blade, fatigue damage, crack propagation.

1. Introduction

In the domain of gas turbine engine lifetime research, it is evident that over 80% of structural damage originates from the turbine component [1]. Consequently, the investigation into fatigue characteristics in the turbine remains critical in the context of gas turbine engines. Especially with expandable turbojet engine, assessment of engine lifetime commonly involves operational hours and start-up cycles [2]. Operational hours entail computations focused on high-cycle fatigue (HCF), employing an analytical approach that evaluates stress produced by blade vibration during engine operation [3] [4]. Conversely, start-up cycles of the engine are linked to computations concerning low-cycle fatigue (LCF), utilizing an analytical methodology that centers on strain produced by the start and shutdown of the engine.

Turbine blades, critical components in aerospace and power generation systems, face intricate challenges during engine start-up, characterized by dynamic loading conditions that significantly impact their structural integrity. Kumal et al. [5] provided a comprehensive analysis through a one-way coupled transient thermal-structural analysis on a three-dimensional model to capture the actual behavior of turbine blade stress during transient operating conditions, enhancing our understanding of stress distributions under realistic operational scenarios. The transient nature of start-up induces complex stress patterns, with peak stresses playing a pivotal role in dictating the initiation and propagation of fatigue-induced cracks. This study focuses on unraveling the intricacies of low-cycle fatigue (LCF) in turbine blades, with a specific emphasis on understanding the initial peak stresses and local plastic strain.

Studies on turbine stress behavior have highlighted the dynamic and multifaceted nature of loading during engine start-up [6] [7]. Notably, the transient thermal loading resulting from fuel ignition and spread across the blade surfaces induces temperature gradients within the structure, influencing the distribution of stresses [8] [9]. Understanding and quantifying the influence of these temperature-

induced stresses on the fatigue life of turbine blades is crucial for enhancing both design and operational considerations.

Furthermore, the combined effects of LCF and HCF are increasingly recognized as critical in assessing the true fatigue life of turbine blades [10]. Stanzl et al. [11] provided an analysis of LCF with the effect of superimposed ultrasonic vibrations in HCF, demonstrating that this combination can rapidly propagate short cracks. Additionally, Shun et al. [12] proposed a new damage accumulation model based on Miner's rule to consider the coupled damage due to HCF-LCF in turbine blades, highlighting the necessity of a comprehensive approach to fatigue analysis.

This paper deals with the low fatigue analysis of turbine blades of a small turbojet engine. The finite element (FE) method is employed to meticulously assess the performance of these turbine blades using ANSYS 2019 software [13]. In an innovative approach, a multi-model strategy is adopted, integrating dynamic inputs sourced from the combustor exit - encompassing thermal and pressure maps. This approach facilitates a transient exploration, unveiling peak stress values across the entire engine test cycle, ranging from initiation to shutdown. The ensuing insights distinctly spotlight heightened stress concentrations at the leading edge, coupled with localized plastic strain precisely at the moment of ignition. The occurrence of such localized plastic deformation on turbine blades may instigate the commencement of initial cracks, thus serving as a precursor to fatigue failure in the turbine blades

In order to quantify the impact of observed local plastic strain on low fatigue life, this study employs the Manson-Coffin equation, providing a predictive framework for estimating the number of cycles to failure [14]. This method is complemented by advanced numerical techniques, such as the Extended Finite Element Method (XFEM) [15] [16], known for its effectiveness in capturing crack propagation [17]. Experimental validations, including Scanning Electron Microscopy (SEM) analysis of fracture surfaces, not only validate numerical simulations but also provide visual evidence of fatigue-related damage. By synthesizing insights from both numerical and experimental approaches, this study aims to contribute to the broader understanding of turbine blade durability.

2. Methodology

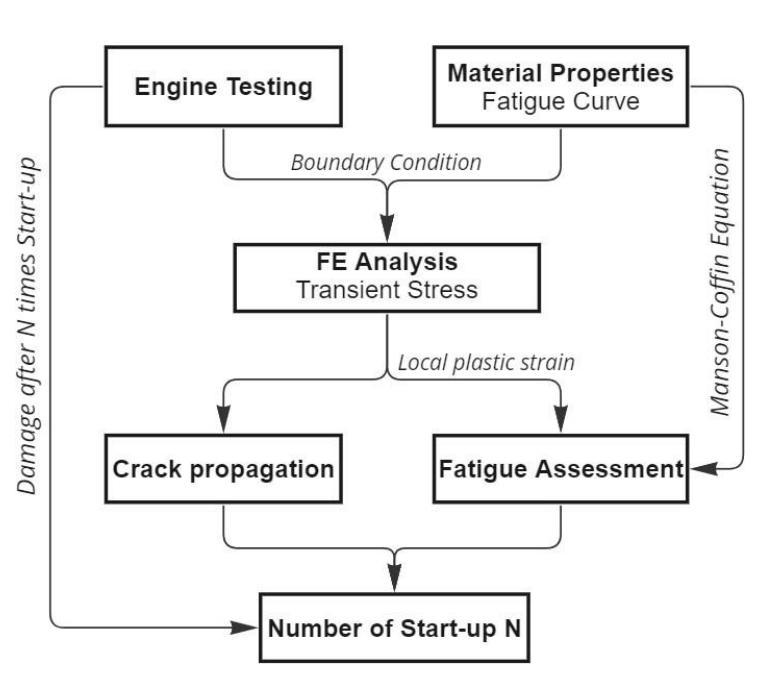


Figure 1 –Schematic diagram of study

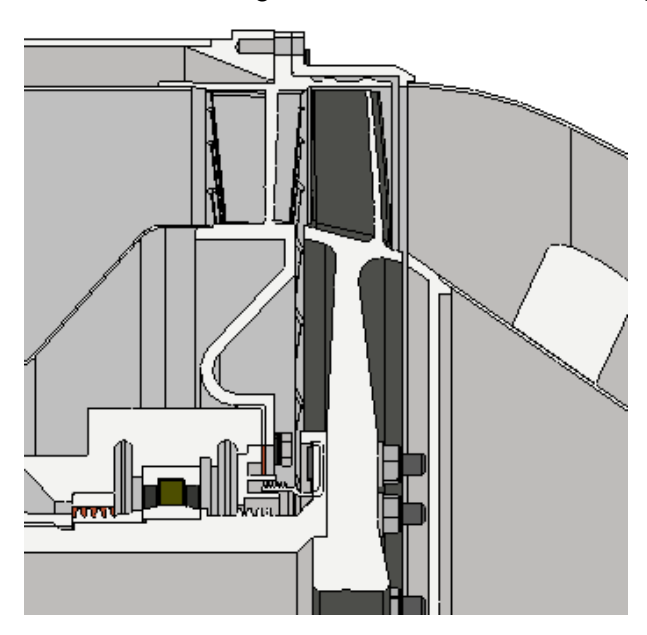
As show in Fig. 1, engine testing data and material properties are employed as inputs for Finite Element (FE) analysis. The FE analysis yields critical stress and local plastic strain. These results, coupled with the fatigue properties of the material and the Manson-Coffin equation, enable the estimation of the number of cycles to failure. Subsequently, the Extended Finite Element Method (XFEM) is applied to simulate crack propagation. After N cycles, the methodology incorporates a comparison between observed signs of damage and numerical calculations, ensuring convergence and enhancing the understanding of turbine blade fatigue behavior.

This systematic approach integrates experimental data, numerical simulations, and analytical methods to provide a comprehensive understanding of the fatigue behavior and damage

progression in turbine blades.

This article examines a small gas turbine engine, which is now undergoing validation testing on the ground. The engine operates at a designed rotation speed of 25,000 RPM and generates an equivalent thrust of 450 kgf designed for manned and unmanned aerial vehicles (UAVs) as well as the target drones. The engine construction consists of five axial compressor stages and a single stage turbine.

The turbine is made of Inconel 718, a durable nickel-chromium alloy known for its superior performance characteristics. The chemical composition and mechanical properties of Inconel 718 are manufactured according to Standard SAE AMS 5663 [18].



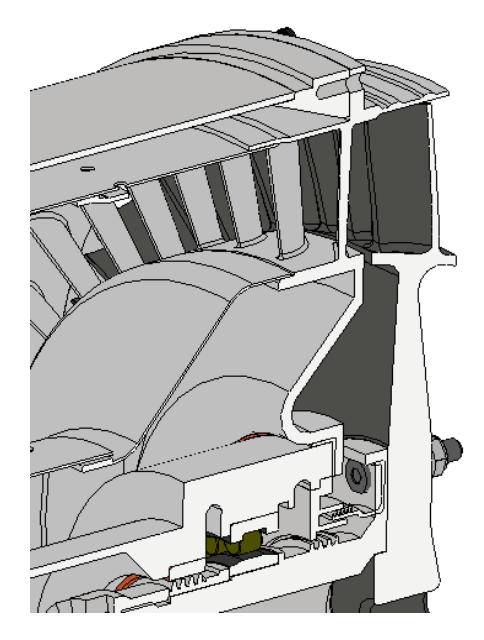


Figure 2 – Turbine component geometry

The geometry includes the turbine stage components, comprising the integrally bladed disc (blisk) and the nozzle guide vane (NGV), as illustrated in Fig. 2. The profile of the blade cross-section and all the dimensions of the blade are defined. Ansys SpaceClaim was utilized to construct the 3D model of the entire geometry.

3. Finite Element Analysis

3.1. Boundary Condition

Utilizing Ansys 2019, the simulation integrates thermal transient, structural transient, and computational fluid dynamics (CFD) investigations into a one-way coupling model.

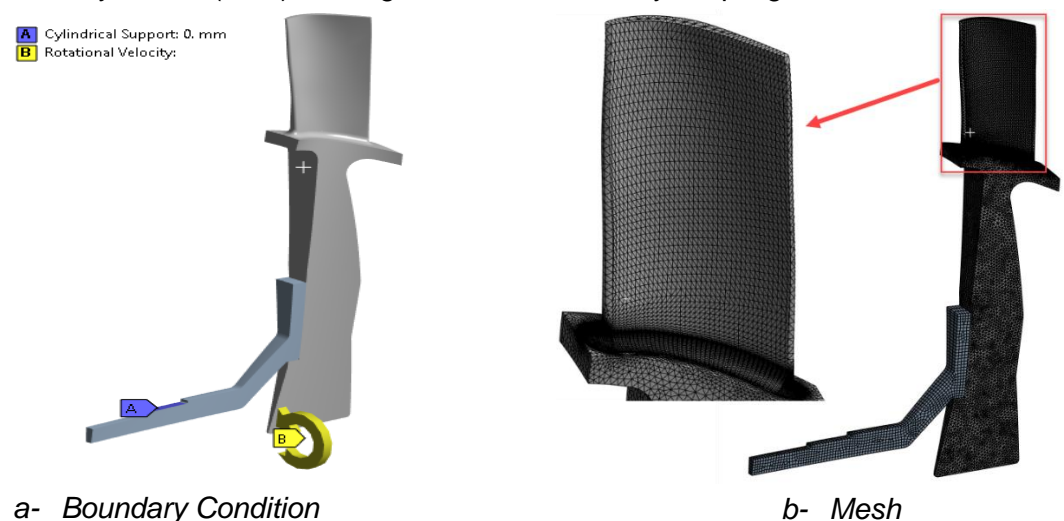


Figure 3 – Turbine blade modeling

Fig. 3 demonstrates the simulation model of a turbine rotor blade, depicting an axisymmetric blade segment instead of the complete circular assembly of the turbine. This segmentation significantly reduces computational requirements. The turbine blade is finely meshed at the blade hub with a

mesh size of 0.2 mm, while the disc section employs a coarser mesh size of 1 mm. The whole model comprises a total of 743,125 mesh elements.

The boundary conditions for the cylindrical ball bearing adopt a cylindrical support configuration, where five degrees of freedom are fixed, and allowing only free axial displacement. The rotational velocity criteria are defined based on the time computed to match the actual test conditions, as shown in Fig. 4.

The engine initiates start-up with the assistance of compressed air, reaching 20% of the designed rotational speed. Prior to ignition, high-pressure fuel is continuously supplied from the combustion chamber and accumulates on the turbine blades.

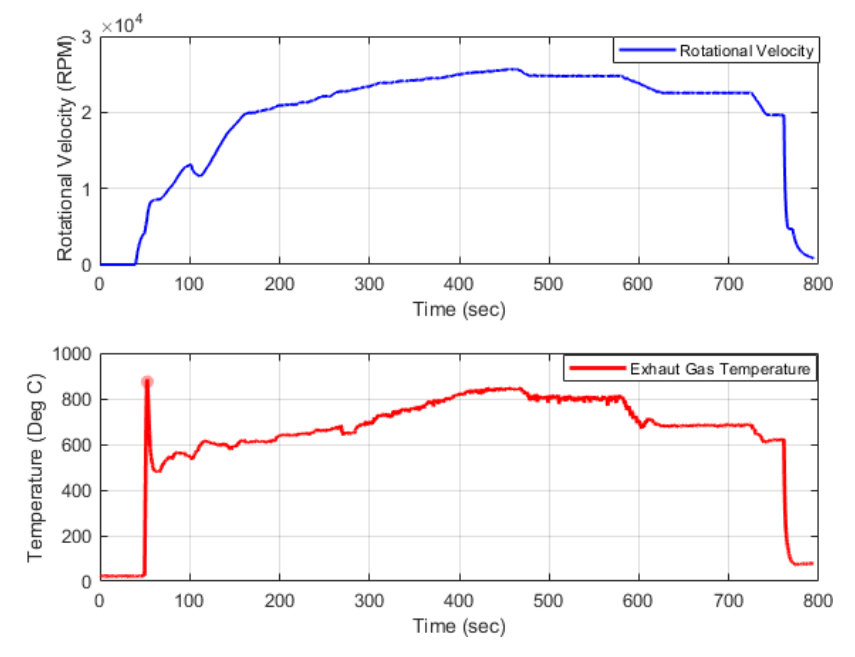


Figure 4 – Boundary condition from actual engine testing data

Fig. 4 illustrates a typical engine test, with the green line representing the rotational speed and the red line representing the exhaust gas temperature (EGT). At the moment of ignition, the accumulated fuel on the turbine blades combusts, causing the temperature on the blade surface to rise to 850 degrees Celsius within approximately 2 seconds. This temperature is recorded by the EGT sensor positioned directly behind the turbine blades. Concurrently, the engine's speed rapidly accelerates to 95% of its designed rotational speed.

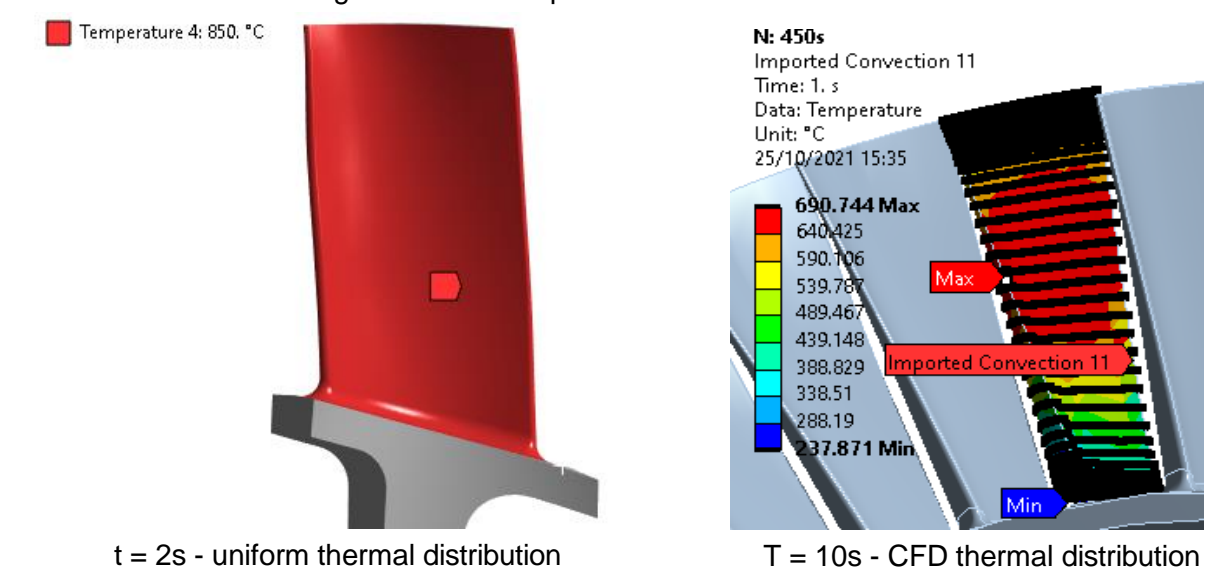


Figure 5 – Thermal condition on blade surface in simulation

The simulation's thermal conditions, which were based on comparable experimental test results, are shown in Fig. 5. In order to simulate the peak temperature caused by the remaining fuel on the blade surface, it is assumed that the temperature is evenly distributed across the blade surface two

seconds after ignition. After this ignition phase, the computational fluid dynamics (CFD) team provides the air temperature produced by the combustor that is used to establish the blade surface temperature.

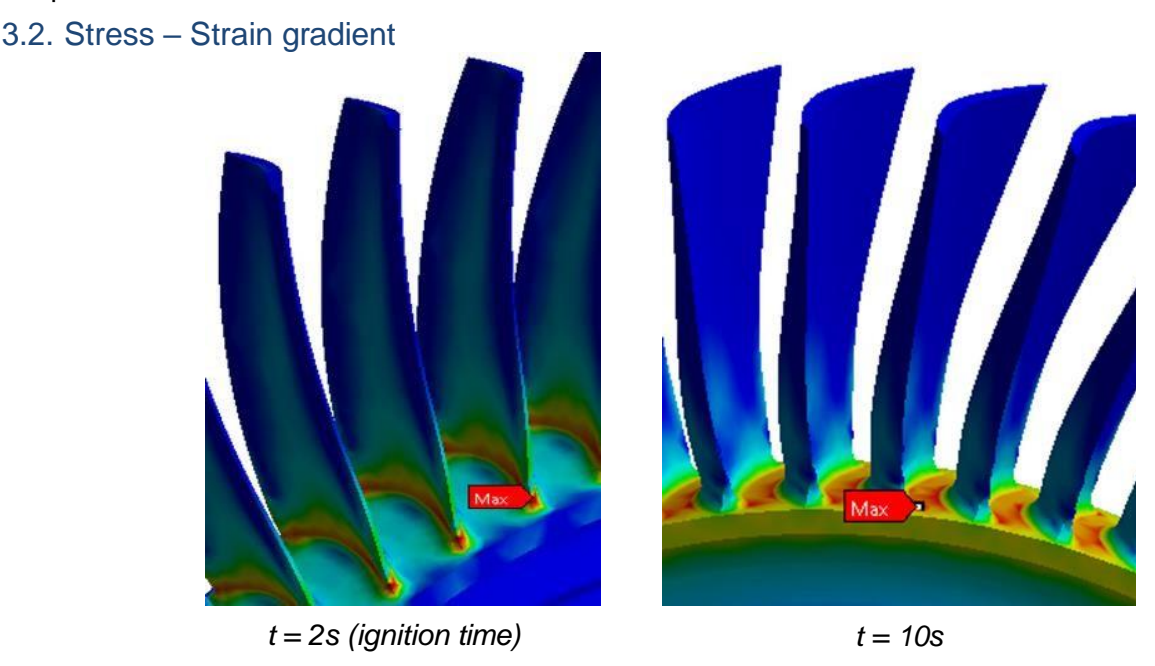


Figure 6 - Turbine blade stress over time

The transient structural model captures the dynamic stress conditions over time. Fig. 6 illustrates the stress levels of the turbine blades at two critical stages: the initial ignition phase and the subsequent post-ignition phase. The thermal gradient is primarily responsible for the high stress levels observed at 2 seconds and 10 seconds. The transient analysis vividly demonstrates the temporal shift in the location of maximum stress on the blade throughout the testing period.

At t=2 seconds after ignition, the blade temperature peaks, resulting in the highest stress at the blade hub, which reaches 805 MPa. This peak stress is attributed to the rapid temperature difference between the blade and the rim disc. As the combustion reaction stabilizes at t=10 seconds, the turbine temperature decreases. The temperature on the blade gradually stabilizes and becomes non-uniformly distributed, transferring from the blade to the turbine disc due to heat transfer and the conductivity of the metal. This thermal redistribution leads to changes in the stress field, induced by thermal stress. Consequently, the maximum stress relocates from the blade base to the point of contact between the blade hub and the disc rim, with a recorded maximum stress of 587 MPa at this stage.

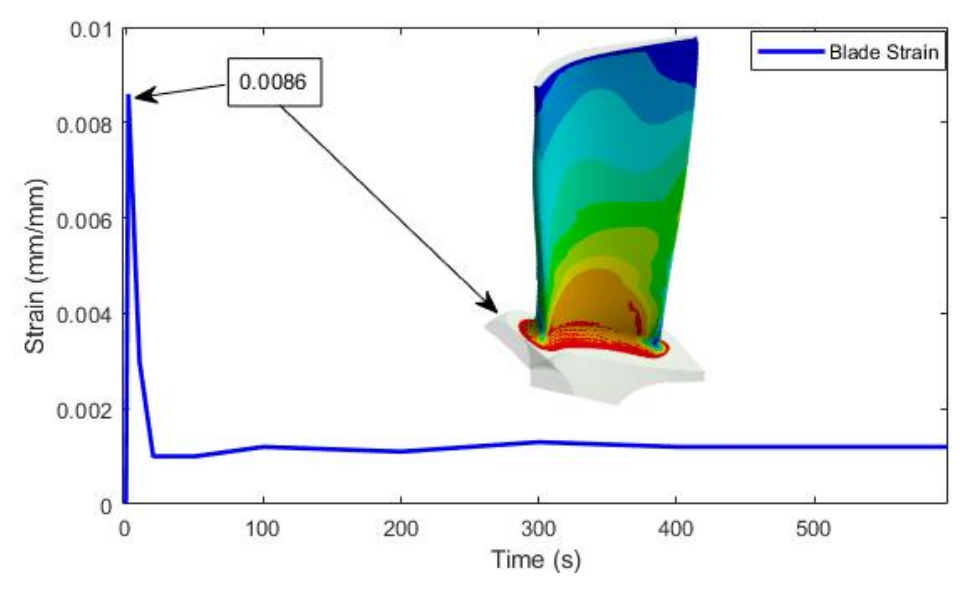


Figure 7 – Turbine blade strain over time

Similar to the stress on the blade, the leading edge root exhibits a peak plastic deformation at the 2-second mark (Fig.7). The recorded value for plastic deformation is noted to be 0.86%. Local plastic strain changes with a large amplitude following each start-up can result in sudden failures if the starting temperature is too high, or the appearance of initial crack. The turbine blade deforms by less than 0.1% after the ignition period once the blade stress stabilizes.

4. Low Cycle Fatigue Assessment

4.1 Analytical - Fatigue Curve

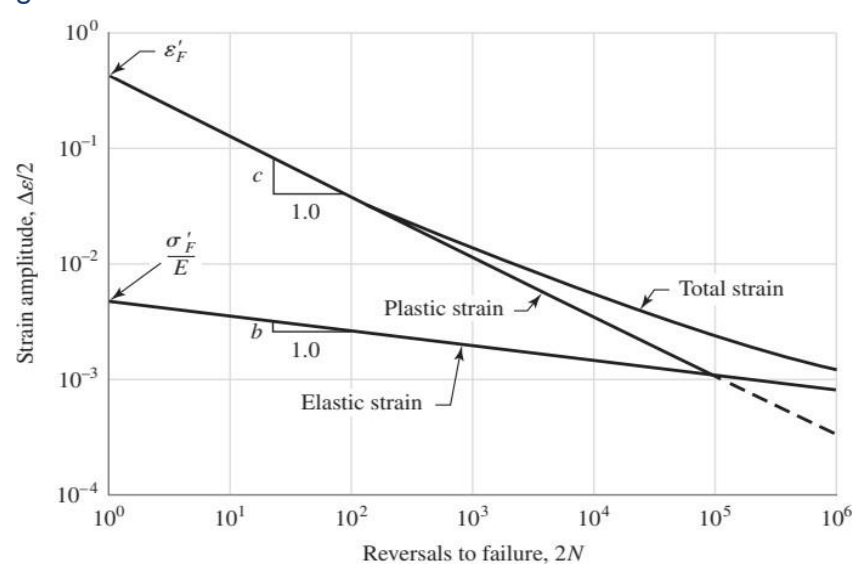


Figure 8 – Fatigue curve – Strain amplitude versus reversal

To acquire fatigue curve data, fatigue strength experiments are conducted by material suppliers. These experiments are performed on cylindrical specimens under strain-controlled conditions following the ASTM E606 standard [19]. Which outlines the procedures for conducting cyclic strain-controlled tests to generate data that characterize the cyclic deformation and fatigue crack initiation behavior of materials.

In the Low-Cycle Fatigue (LCF) analysis, the Manson-Coffin method stands as the most widely applied approach [20]. The number of fatigue cycles can be computed using the respective equation:

$$\varepsilon p = \varepsilon' f(2N)^c \tag{1}$$

 ε'_f – fatique ductility component

c – fatigue ductility exponent

 ε_p – the plastic strain amplitude

Table 1: Fatigue properties of Inconel 718 AMS 5663

	fatigue ductility component	plastic strain amplitude	fatigue ductility exponent	Number of cycle
	ε' _f	$oldsymbol{arepsilon}_{ ho}$	C	N
Inconel 718	0.22	0.0086	-0.75	56

Fatigue testing, conducted in accordance with ASTM E606 standards, is employed to determine both the fatigue ductility coefficient and the fatigue ductility exponent. These tests are conducted within a temperature range of 650°C to 850°C, which closely simulates the operational conditions of the engine. At elevated temperatures, the mechanical properties of Inconel 718 change, often increasing ductility and decreasing yield strength.

A higher fatigue ductility component aligns with these observations, indicating the material's enhanced ability to deform plastically at high temperatures. Regarding the fatigue ductility exponent, this parameter in the Manson-Coffin equation represents the relationship between the number of cycles to failure and the plastic strain amplitude as shown in Fig. 8. A negative value of c indicates that as the plastic strain amplitude increases, the number of cycles to failure decreases logarithmically.

With an average plastic strain amplitude of 0.86% derived from finite element analysis, the number

of test cycles according to the Manson-Coffin formula is determined to be 56 cycles.

4.2 Crack Propagation Simulation

The crack propagation problem is simulated using the ANSYS Extended Finite Element Method (XFEM) module. The initial fracture is assumed to occur at the node where the predicted plastic stress is highest.

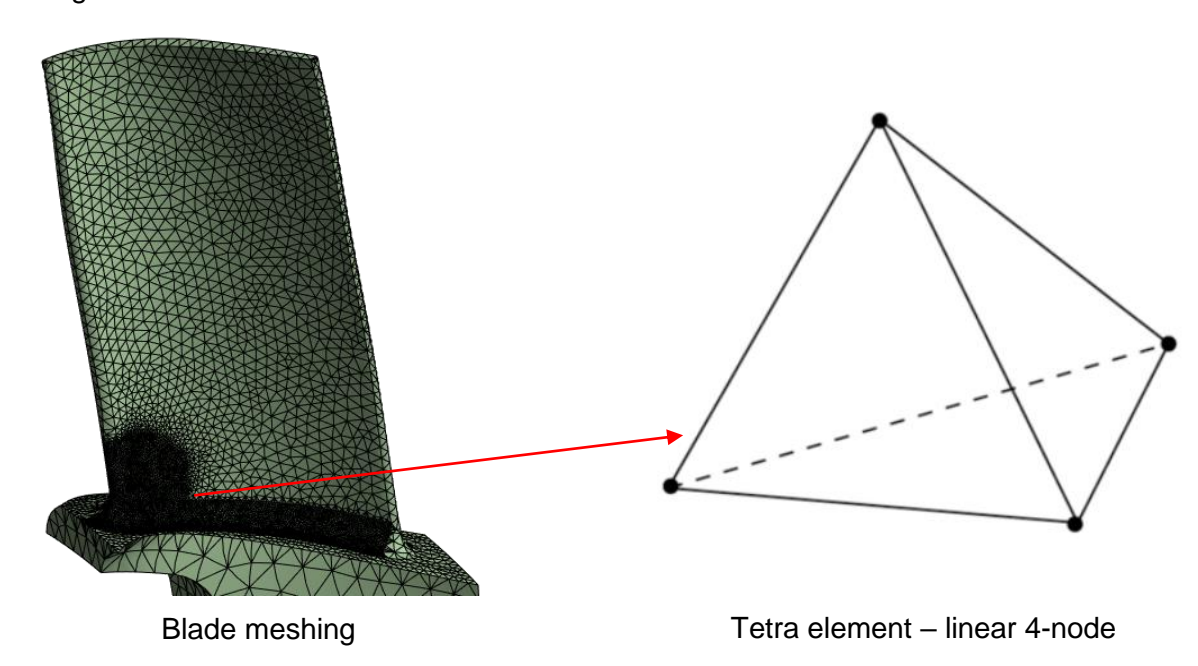


Figure 9 – Blade meshing for XFEM analysis

The simulation of crack propagation using the Extended Finite Element Method (XFEM) necessitates the use of extremely fine meshes, particularly at the initial crack location to accurately capture the stress intensity factors and crack growth behavior. In this study, a sphere meshing technique is employed to achieve the required mesh refinement in the region of interest, as illustrated in Fig. 9.

The static analysis of the structure was performed using a 4D20 hexagonal (HEX) lattice, which provides a robust framework for general structural analysis due to its high information-carrying capacity per element. However, in the context of crack propagation simulation, the HEX lattice is insufficient for capturing the nuanced details required for accurate results. For crack propagation analysis, the use of tetrahedral mesh elements, specifically C3D4 elements, is well-recognized for its superior accuracy. This mesh type is particularly advantageous for modeling crack growth as it effectively captures the singularity at the crack tip, which is critical for understanding the stress intensity factors and crack progression. The C3D4 tetrahedral elements facilitate a more precise simulation of the crack propagation process, ensuring that the stress and deformation fields around the crack tip are accurately represented.

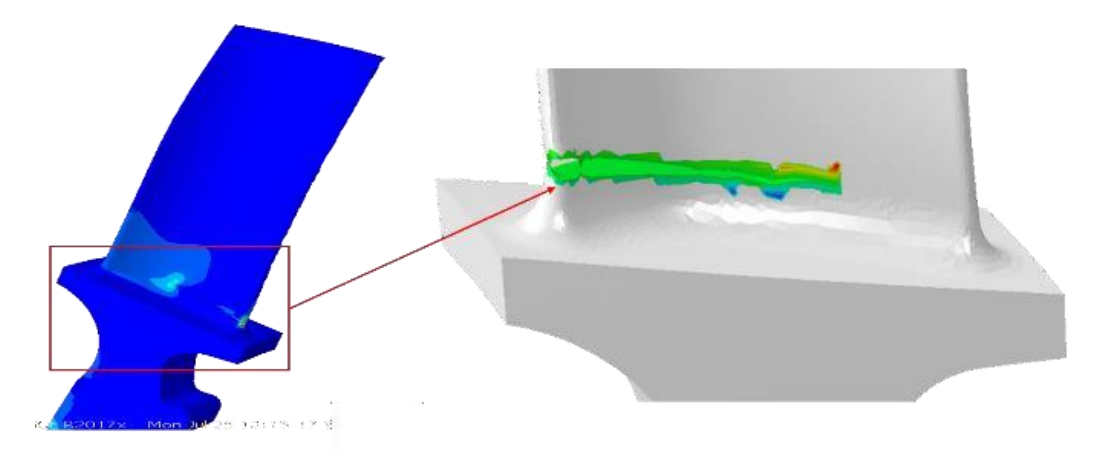
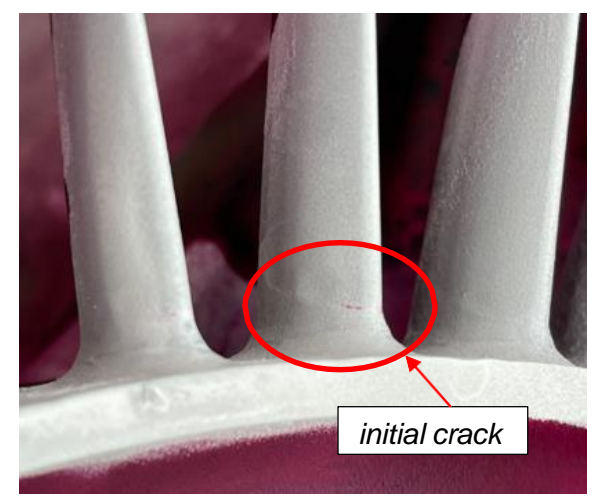


Figure 10 – Crack propagation simulation

Examining the locations exhibiting initial plastic strain, the XFEM method simulates the initiation and propagation of cracks under the operational conditions of the engine. The cracks exhibit a tendency to propagate horizontally along the blade root.

5. Engine Testing Validation

In the course of ground engine testing, a meticulous examination and assessment of turbine blades is systematically conducted subsequent to each testing iteration. The methodologies employed for crack inspection encompass Liquid Penetrant Testing (LPT) and the Eddy Current Method (ECM).





Initial crack

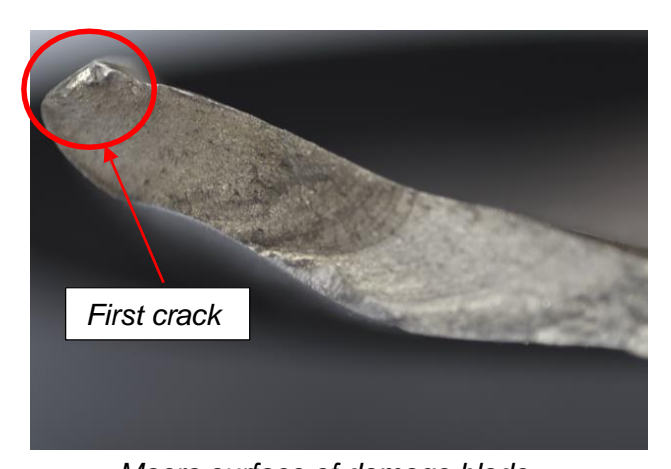
Crack propagated after 49 times of start-up

Figure 11 – The initial crack at leading edge

The turbine blades were subjected to a series of rigorous tests, with periodic inspections conducted to assess their structural integrity. Up to the 40th test, no abnormalities or defects were observed in the turbine blades. However, post-test inspection following the 40th test revealed a small crack on one of the blades, as detected using the PT method, illustrated in Fig. 11. As testing progressed, the incidence of cracks increased significantly; by the 49th test, cracks were detected in 11 out of 53 blades. This progressive damage underscores the importance of continuous monitoring and detailed inspection to prevent catastrophic failure.







Macro surface of damage blade

Figure 12 – Low cycle fatigue damage in turbine blade

The rate of crack propagation increased significantly, and during the 52nd test cycle, one turbine blade completely ruptured as shown in Fig. 12. Macroscopic examination of the damaged cross-sectional area provided clear evidence of fatigue-related failure. These macroscopic images distinctly displayed fatigue striations and crack propagation patterns, characteristic of fatigue failure under cyclic loading conditions.

The numerical simulations had predicted the fatigue life of the turbine blades to be 56 cycles. The experimental observation of complete blade failure at 52 cycles indicates a close correlation

between the simulated and experimental results. This minimal disparity between the predicted (56 cycles) and observed (52 cycles) fatigue lives underscores the reliability and accuracy of the numerical models used.

The high fidelity of the simulation in predicting the fatigue life highlights its utility in preemptively identifying potential failure points and improving the design and maintenance schedules for turbine blades. The alignment between the numerical and experimental results reinforces confidence in the methodologies employed for fatigue life estimation and provides valuable insights into the material behavior under cyclic thermal and mechanical loads.

6. Conclusion

The research intended to investigate the fatigue response of an expandable turbojet engine's turbine blade in terms of low cycle fatigue. The primary objective is to develop a computational approach for calculating engine start-up cycles based on engine reality test data at ground level. Stress concentration at the root of blade's leading edge post-ignition is analyzed using the finite element method and assessed by fatigue theory.

- Peak temperature and local plastic strain: The phenomenon of peak temperature on the blade surface due to high fuel pressure before ignition in single-event engine configurations can lead to the occurrence of plastic strain at the blade root. This is one of the key factors limiting the number of engine test cycles, particularly during ground-level testing.
- Complex Stress Analysis: The complex stress state of the turbine blade was effectively analyzed through transient FEM analysis, capturing local plastic strain at the leading edge.
 These outcomes are unattainable with steady-state analysis alone, underscoring the necessity of transient analysis for accurate stress and strain assessment
- Fatigue life estimation: The plastic strain at the leading edge's root serves as input for calculating the limit of engine start-up cycles with the Manson Coffin equation and the Paris Law fatigue theory. The deviation between the numerical calculated and experimental outcomes is not markedly substantial. This result underscores the convergence and reliability of the finite element method and the Manson-Coffin fatigue life evaluation equation.
- Crack propagation: The development trends of crack propagation and damage marks at the blade's leading edge converge with the predicted results of crack propagation from XFEM analysis.

Overall, this comprehensive analysis provides valuable insights into the fatigue behavior of gas turbine engine blades. It contributes to a more accurate understanding of the engine's operational limitations and enhances the reliability of predictive maintenance strategies.

The results underscore the importance of integrating advanced numerical methods with experimental validation to improve the design and longevity of turbine blades in high-stress environments.

7. Contact Author Email Address

Mailto: minhhn5@viettel.com.vn or nhatminhcdpk52@gmail.com

8. Copyright Statement

The authors confirm that they, and/or their company or organization, hold copyright on all of the original material included in this paper. The authors also confirm that they have obtained permission, from the copyright holder of any third party material included in this paper, to publish it as part of their paper. The authors confirm that they give permission, or have obtained permission from the copyright holder of this paper, for the publication and distribution of this paper as part of the ICAS proceedings or as individual off-prints from the proceedings.

References

- [1] Lewis Center, "Factor That Affect Operational Realiability of Turbojet Engines," National Aeronautics and Space Administration (NASA), 1960.
- [2] M. Boyce, GasTurbine Engineering Handbook, 1982.
- [3] Jörg R. Riccius and Evgeny B. Zametaev, "HCF and LCF Analysis of a Generic Full Admission Turbine Blade," *Aerospace Journal*, vol. 10, no. 2, 2023.
- [4] A. J. Scalzo, "High-Cycle Fatigue Design Evolution and Experience of Free-Standing Combustion Turbine Blades," *Gas Turbine and Aeroengine Congress and Exposition*, vol. 114, pp. 284-292, 1991.
- [5] Rahul Kumar, V. S Kurmar, M. Butt, "Thermo-mechanical Analysis and Estimation of Turbine Blade Tip Clearance of a Small Gas Turbine Engine under Transient Operating Conditions," *Applied Thermal Engineering*, 2020.
- [6] Schwerdt, L., Hauptmann, T., Kunin, A., Seume, J. R., Wallaschek, J., Wriggers, "Aerodynamical and Structural Analysis of Operationally Used Turbine Blades," *Procedia CIRP*, vol. 59, p. 77–82, 2017.
- [7] Jae-Hoon Kima, Ho-Young Yanga and Keun-Bong Yoo, "A Study on Life Prediction of Low Cycle Fatigue in Superalloy for Gas Turbine Blades," vol. 10, pp. 1997-2002, 2011.
- [8] Feng Li, Zhao Liu, Zhenping Feng, "Experimental and computational assessment into the heat transfer for the blade multicavity tips," vol. 230, 2023.
- [9] P. Ning Xu, "Transient thermal stress analysis of the typical structures in turbine rotor based on thermomechanical analysis," *TurboExpo ASME*, 2014.
- [10] D. Nowell, Pierrangelo Duó, "Prediction of Fatigue Performance in Gas Turbine Blades after Foreign Object Damage," *International Journal of Fatigue*, vol. 25, no. 9, pp. 963-969, 2003.
- [11] S.E. Stanzl-Tschegg, M. Meischel, A. Arcari, N. Iyyer, N. Apetre, N. Phan, "Combined cycle fatigue of 7075 aluminum alloy Fracture surface characterization and short crack propagation," *International Journal of Fatigue*, vol. 91, pp. 352-362, 2016.
- [12] Shun-Peng Zhu, Peng Yue, Zheng-Yong Yu and Qingyuan Wang, "A Combine High and Low Cycle Fatigue Model for Life Prediction of Turbine Blades," *Materials*, vol. 10, 2017.
- [13] ANSYS Inc, "ANSYS Mechanical Tutorial," Canonsburg, 2019.
- [14] Julie A. Bannatine, Jess J. Comer, Jame L. Handrock, Fundamental of Metal Fatigue Analysis, 1990.
- [15] H. Bayesteh, S. Mohammadi, "XFEM fracture analysis of shells: The effect of crack tip enrichments," *Computational Materials Science*, vol. 50, no. 10, pp. 2793-2813, 2011.
- [16] E. Chatzi, "Introduction to the Extended Finite Element Method," *Structural Mechanical*.
- [17] Lucjan Witek, "Numerical Simulation of Fatique Fracture of the Turbine Disc," *Fatigue of Aircaft Structures*, vol. 1, pp. 114-122, 2012.
- [18] Aerospace Material Specification AMS 5663, "Nickel Alloy, Corrosion And Heat-Resistant, Bars, Forgings, And Rings 52.5Ni 19Cr 3.0Mo 5.1Cb (Nb) 0.90Ti 0.50Al 18Fe Consumable Electrode Or Vacuum Induction Melted 1775 °F (968 °C) Solution And Precipitation Heat Treated," SAE Aerospace, 2004.
- [19] ASTM 606, Standard Test Method for Strain-Controlled Fatigue Testing, 2021.
- [20] D. Fournier, Andre Pineau, "Low cycle fatigue behavior of Inconel 718 at 298 K and 823 K," *Metallurgical and Materials Transactions*, vol. 8, pp. 1095-1105, 1977.